Functional Electron Microscopy for Electrochemistry Research: From the Atomic to the Micro Scale

by Albina Y. Borisevich, Miaofang Chi, and Ray Unocic

The operation of batteries, fuel cells, and other energy storage and conversion devices is underpinned by the intricate synergy of ion transport, phase transformations, and electrochemical reactions. While electrochemical processes in well-defined molecular systems are amenable to classical chemical techniques including *in situ* optical spectroscopies and nuclear magnetic resonance (NMR), phase transformations and reactivity in solids and at solid interfaces remain largely an enigma. The presence of multiple types of structural defects and imperfections, competing electron and ion transport pathways, and multiple possible surface reconstruction types, combined with the directionality of ion flows and state of charge transformation fronts render these phenomena inaccessible to macroscopic interrogation techniques. At the same time, knowledge of the individual mechanisms involved in electrochemical reactivity of solids at the level of individual, atomic size structural elements is required for understanding the fundamental mechanisms of energy storage, factors controlling charge/discharge rates, degradation and failure processes, and ultimately knowledge-driven prediction and optimization of energy materials.[1-3]

In the last 15 years, a number of remarkable breakthroughs in aberration correction in the transmission electron microscope (TEM) and scanning transmission electron microscope (STEM) have opened possibilities for sub-angstrom characterization of materials, both from structural and chemical points of view (see schematic of a STEM in the center of Fig.1). With achievable resolution as low as 0.5 Å,[4] imaging single atoms became routine, and it became possible to *identify* a single atom both from imaging[5] and from spectroscopic signals.[6,7] For crystals, collection of two-dimensional, atomic resolution chemical maps became feasible,[8,9] and imaging of light element columns such as lithium[10,11] and even hydrogen[12] has been reported.

Alongside these developments in the world of ultra-high resolution, there has been remarkable development in a variety of *in situ* techniques and platforms enabling observation of dynamic processes under a variety of external stimuli inside an electron microscope. The progress made is evident, and is manifested in the advances in *in situ* mechanical testing of micro- and nanoscale objects,[13-15] in studies of heterogeneous catalysts at elevated temperatures and in gaseous atmosphere while preserving high resolution,[16-18] and in imaging of processes occurring in liquids[19]. Another growth area within the *in situ* electron microscopy field involves the application of bias inside the microscope. A variety of approaches have been reported, from uniform biasing of specially fabricated specimens[20] to using a setup with a moveable tip to apply the bias locally.[21,22] While most of the results reported thus far deal with ferroelectric switching, materials such as oxygen conductors[23] and resistive memories[24] can also be characterized using *in situ* biasing. An especially interesting variation involves the use of vacuum-compatible ionic liquids.[25]

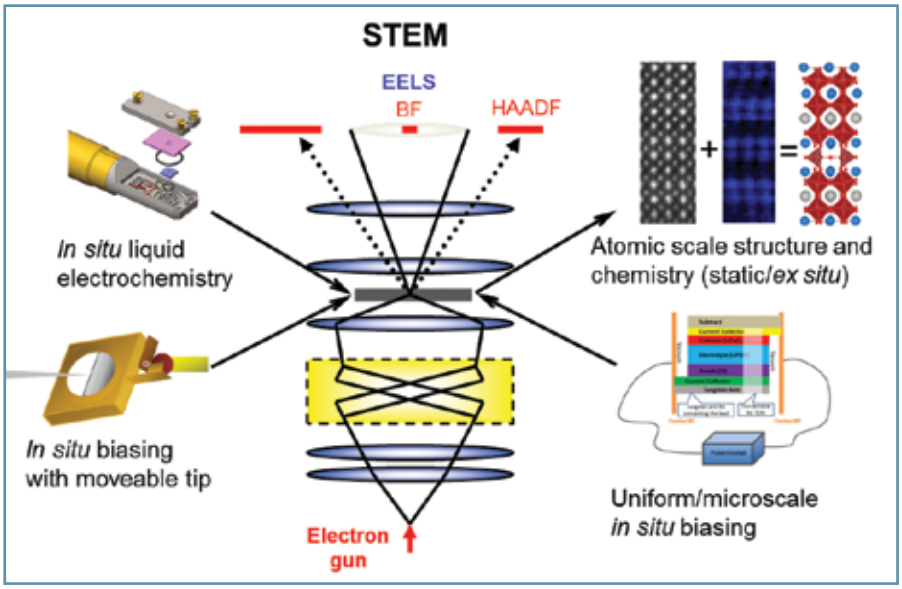

Fig. 1. *(Aberration corrected) STEM: a variety of detectors and experimental approaches.*

In this article, we present the possibilities that STEM and electron energy loss spectroscopy (EELS) offer in terms of probing fundamental aspects of electrochemical systems by combining electron microscopy with *in situ* control of local electrochemical potentials by tuning the atmosphere, by biasing, or using a liquid environment. A graphical summary of the available methods is given in Fig.1, with several examples below. The examples discussed herein will follow Fig. 1 clockwise from the upper right, starting with high resolution investigations in static or *ex situ* conditions and ending with *in situ* electrochemical liquid cell studies.

One of the beneficial consequences of the higher resolution of the aberration-corrected microscopes has been a marked improvement in signal to noise ratio of the images, enabling detection of structural distortions down to the single picometers level. This capability was most extensively utilized to probe ferroelectric materials, where off-center displacements of metal cations in the unit cell are directly related to ferroelectric polarization.[26-30] However, the same capability can be utilized for atomic-level studies of the oxygen conducting oxides used in solid oxide fuel cells based on their chemical expansivity behavior. Chemical expansivity refers to the expansion of some oxygen conducting materials in a reducing atmosphere and is well known in the field of solid state electrochemistry.[31] Their expansion scales linearly with the log of oxygen partial pressure and can be detected dilatometrically.[31,32] In Ref. [33], Kim and coworkers have demonstrated that the concept of chemical expansivity can be extended all the way to atomic level, showing that local lattice spacings measured from high-angle annular dark-field (HAADF) STEM images are linearly related to the local oxygen content. They studied $La_{0.5}Sr_{0.5}CoO_{3-\delta}$ (LSCO) thin films on lanthanum strontium aluminum tantalate (LSAT) and neodymium gallate (NGO) substrates. Both films demonstrated lattice parameter modulations; EELS studies were used to show that the modulation was associated with oxygen vacancy ordering, with larger local lattice spacing corresponding to an oxygen-depleted layer (Fig. 2a). The LSCO/NGO film was identified as brownmillerite $La_{0.5}Sr_{0.5}CoO_{2.5}$ via a detailed structural study, while the observed chemical expansion in LSCO/LSAT film was lower. First principles calculations were

(continued on next page)

then used to demonstrate that local lattice spacing changes increased linearly with the number of oxygen vacancies. The results of the calculations, which matched very well with experimental measurements of layer spacings in $La_{0.5}Sr_{0.5}CoO_{2.5}$, were then used as a calibration curve to recalculate lattice spacings into a local oxygen content (Fig. 2b, c). From this interpretation, the average composition of the LSCO/LSAT thin film was determined to be $La_{0.5}Sr_{0.5}CoO_{2.75}$. This film showed considerable local inhomogeneity, highlighting the capabilities of the method to detect both global composition and local variations.[33]

Distribution of oxygen vacancies and the emergence of vacancy ordering are of critical importance to ionic conductivity,[2] and changes in the vacancy distribution under a given operating condition can have a profound effect on the longevity of the material. While the fine structural analysis used by Kim *et al*.[33] is not yet feasible under bias or other realistic conditions, *ex situ* studies, when materials are being investigated before and after external stimuli are applied, can provide initial insights. Recently, Leonard *et al*.[34] used Electrochemical Strain Microscopy (ESM)[35] to subject different areas of the $La_{0.8}Sr_{0.2}CoO_{3-\delta}$ (LSCO) thin film on yttria stabilized zirconia to bias cycling with different amplitudes. The deformation hysteresis loops resulting from the cycling were recorded. Additionally, bias cycling produced visible and irreversible deformation of the surface, the extent of which varied with the amplitude of the bias applied (see AFM image in Fig. 2d). To examine the nature of the structural changes, a focused ion beam was used to make a STEM specimen with individually addressable windows for each applied bias value (Fig. 2e). Most of the visible deformation was attributed to surface amorphization and the formation of voids; however, changes to the crystalline structure as a function of bias were also detected. Fig. 2f shows a HAADF STEM image of LSCO crystal lattice showing some lattice modulation, using the same approach as Kim *et al*.[36] The spacing map derived from the area in the red square shows that the ordering is not homogeneous. Leonard *et al*. collected a sampling of such maps for regions for each value of bias amplitude. Using the average difference between high and low lattice spacings as a measure of the degree of order,

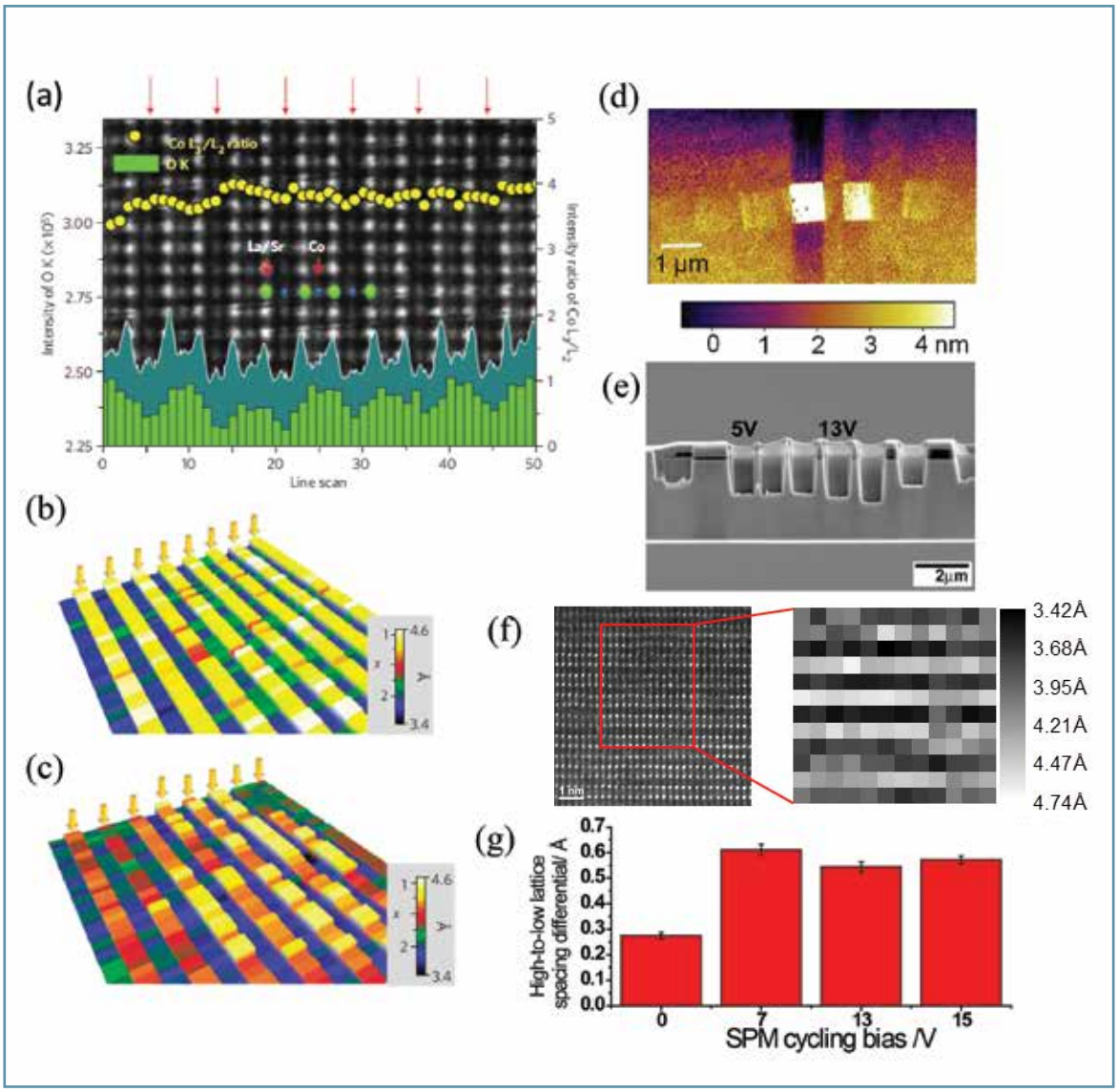

Fig. 2. *Oxygen vacancy mapping at high resolution (a) HAADF image of a vacancy ordered LSCO film, with overlapping HAADF profile (teal) and O K EELS edge intensity profile (green); oxygen depleted planes are highlighted with arrows. (b, c) Lattice spacing/ local oxygen concentration maps for (b) LSCO/NGO and (c) LSCO/LSAT films, illustrating differences in overall oxygen concentration and local degree of disorder. (d) AFM topography image of an LSCO thin film after bias cycling at (left to right) 5 V, 9 V, 15 V, 13 V, and 11 V respectively. (e) SE micrograph of STEM sample after FIB final thinning of ESM bias cycled regions. (f) A typical STEM image of a vacancy ordered region of LSCO thin film and the lattice spacing map computed from the region in the red box. (g) The difference between the highest and the lowest spacings in maps such as Fig. 2f for areas cycled at different bias values (adapted from Refs. 33,34).*

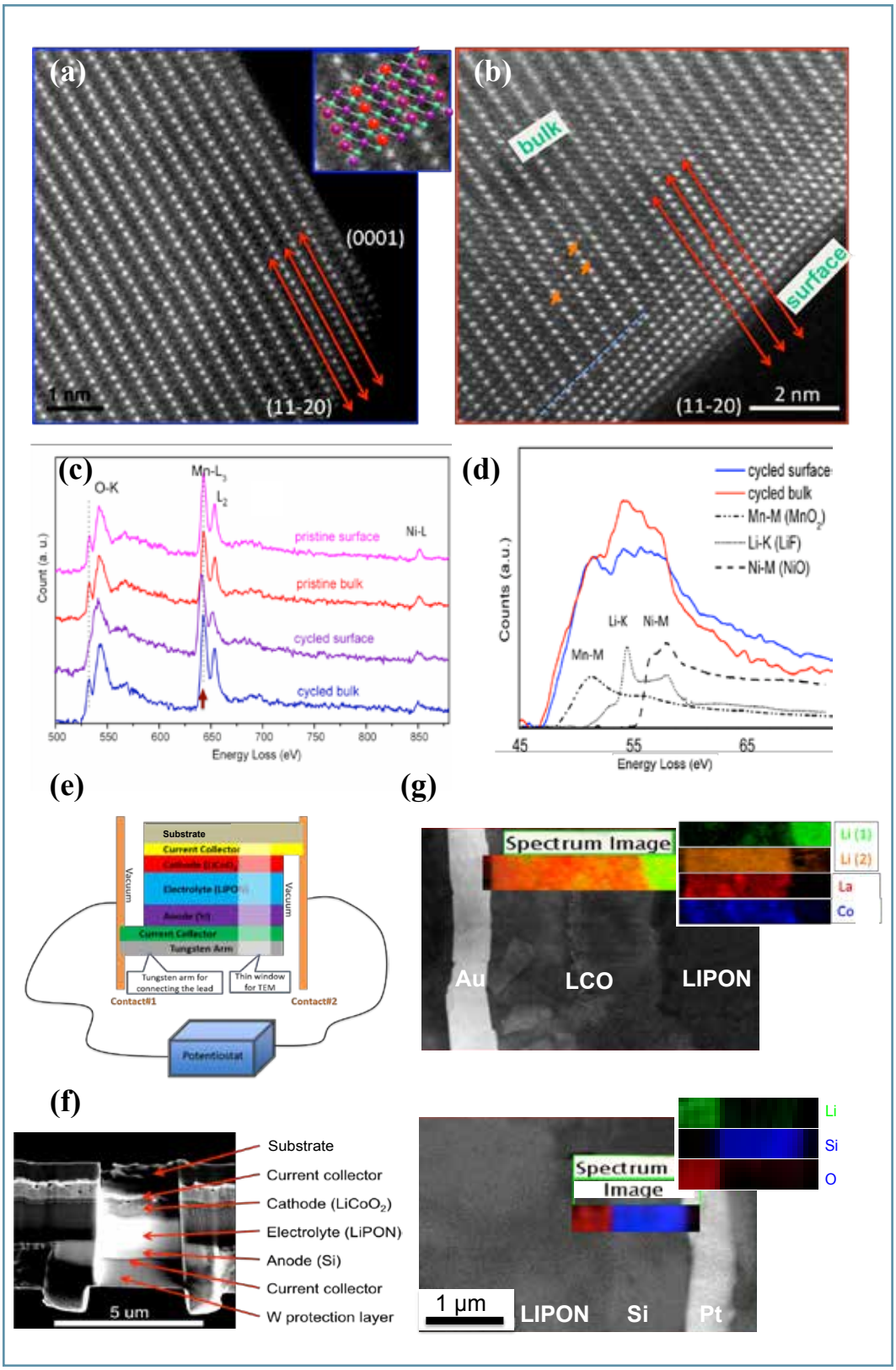

Fig. 3. *(a, b) Atomic resolution Z-contrast images of pristine (a) and after 10 cycles (2-4.8V) (b) of Li-rich layered $Li[Ni_{1/5}Li_{1/5}Mn_{3/5}]O_2$ grains along the [100] zone axis. The surface structural transformation due to TM ions migration to lithium sites after cycling partially blocks the Li transport pathway, as schematically shown by dashed arrows; small orange arrows show observed TM migration in grain bulk (less pronounced than at the surface). (c) EELS fine structures of O-K and Mn-L edges proves the surface structural transformation. (d) Li-K edge spectra show significant Li loss at the surface of cycled particles. EELS spectra of MnO_2, LiF and NiO used for MLLS fitting are also displayed for reference. (e) The schematic of low-noise, high-stability biasing stage developed for in situ atomic resolution imaging and spectroscopy upon electrochemical cycling in all-solid-batteries. (f) TEM image of the e- beam transparent window before cycling (g), and elemental maps of each component after one charge-discharge cycle inside an electron microscope between 1.5-3.6V (panels a-d adapted from Ref.37).*

they showed that the degree of order increased after bias cycling, however the increase was independent of the bias amplitude (Fig. 2g). This finding suggests that vacancy ordering is thermodynamically favorable, however kinetically hindered under the growth conditions. Bias cycling effectively "anneals" vacancies to the favorable ordered state.

Of equal interest are the atomic-scale investigations of structural and electronic structures of materials for lithium-ion batteries (LIB). The presence of mobile (at room temperature) ions in these materials renders them extremely sensitive to the electron beam. Recently it has been demonstrated that the combination of Z-contrast imaging and EELS is an ideal technique for studying cycling or degradation mechanisms of LIB electrode materials, especially for cathodes based on transition metal intercalation oxides. These materials consist of a largely unchangeable host with specific sites wherein Li ions intercalate. While charging, Li ions are extracted from the cathode host and solvate into and move through the non-aqueous electrolytes. The charge balance during Li extraction is retained by the oxidation of transition metal(s) in the material. During discharge, lithium ions are expected to insert back to the lattice frame fully while the transition metal(s) is/are reduced to their original states. The structural and chemical stabilities of the material at the atomic/ionic scale upon electrochemical cycling thus heavily affects its reversible capacity and operating voltage, which directly determines the energy density and longevity of the LIB.

Recent electron microscopy studies have revealed unexpected structural and chemical evolutions at atomic-scale, which can rarely be detected by other characterization techniques.[37-45] As an example of such work, Fig. 3a-d

(continued on next page)

delineates the atomic structure and chemical evolution upon electrochemical cycling of $Li[Ni_{1/5}Li_{1/5}Mn_{3/5}]O_2$ grains that belong to the family of Li-excess layered oxide compounds used as high voltage cathode materials. The Z-contrast images and EELS fine structures of the pristine material were compared with one that had undergone 10 charge-discharge cycles (2-4.8 V).[37] While the crystal structure retains alternating layer characteristics in the bulk of the grain, the grain surface undergoes phase transformation to a defective spinel structure, evidenced by atomic scale Z-contrast imaging (Fig. 3a, b). The significantly increased contrast at Li layers indicates the migration of a large amount of transition metal ions to lithium sites. This result is further confirmed by high resolution EELS, where a dramatic drop of the O-K edge and the reduction of the Mn valence state are revealed at the surface region of the cycled grains (Fig. 3c). Correspondingly, the Li concentration is reduced by 40%, as quantified by the analysis of the EELS spectra (Fig. 3d). The transition metal ions that enter the lithium layer are not removable during subsequent cycling and hence partially block the lithium diffusion pathways. Such interfacial atomic structure transformation may be one of the factors that cause the intrinsically poor rate capability of this series of materials and the low Li chemical diffusion coefficient in the platueau region during delithiation.[37] This work paves the way for exploring potential surface modification strategies, such as local coating and doping, to optimize the structural and electrochemical performance of this (and similar) series of materials.

The combination of Z-contrast imaging and EELS analysis provides exclusive *local* and *quantitative* information on material composition and structure up to atomic scale. However, to provide a thorough understanding of the microstructural and compositional evolution during every critical charge transfer and transport process in battery materials, *in situ* electron microscopy has to be developed and coupled with *ex situ* characterization. Most of the current efforts on *in situ* microscopy for battery research have focused on tip-based biasing or liquid-cell based configurations. These *in situ* studies have greatly promoted the capability of electron microscopy in terms of directly observing the microstructural evolution in battery systems.[46-48] However, atomic-scale investigations, such as local chemical analysis and atomic-resolution Z-contrast imaging are still very challenging under operando conditions because of (1) a limited stage stability of currently available biasing holders, (2) intrinsic restrictions in configuring a full-cell nanobattery that allows practical electrochemical cycling, and/or (3) the inherent limitations of spatial and energy resolutions due to electron scattering through the membrane and solution in liquid cell-based devices.

We recently developed an *in situ* biasing stage based on direct connection of an all-solid nanobattery to two fixed contacts, providing a relatively robust design for *in situ* TEM observations at atomic resolution. The schematic of the design is shown in Fig. 3e. Such design allows the combination of *in situ* analysis with a complete suite of advanced electron microscopy techniques such as atomic-resolution imaging, EELS analysis and diffraction, which are difficult to achieve with other existing *in situ* TEM setups. This configuration is believed to enable direct observation of Li diffusion, transition metal valence alteration, and composition/structural evolution over a wide length scale, from μm to Å, under electrochemical bias.

This approach was demonstrated via *in situ* studies of an active battery structure as illustrated in Fig. 3f-g, depicting elemental maps of each component in the nanobattery after one charge-discharge cycle inside an electron microscope between 1.5-3.6 V. This nanobattery was composed of Al_2O_3 (substrate), Au (current collector), $LiCoO_2$ (cathode), LIPON (lithium phosphorus oxynitride, electrolyte), Si (anode), Pt (current collector), and W (FIB protective layer). EELS spectrum-imaging was performed to monitor lithium migration and transition metal oxidizing/reducing characteristics during cycling. Detailed dynamic electronic structural evolution of each component can be investigated using such a configuration. For example, as shown in Fig. 3g, the lithium in LIPON can be differentiated from that in $LiCoO_2$ by selecting their characteristic fingerprints in the EELS fine structure. It is important to point out that further improvements of such *in situ* stages (in terms of stage titling flexibility, stability, and the incorporation of cooling and vacuum-transfer systems) are needed for atomic-resolution studies in battery research.

A variety of *in situ* TEM characterization platforms have been developed and recently utilized to probe electrochemical processes in real time and with high spatial resolution in terms of structural and chemical changes as a result of electrical stimuli. These electrochemical measurement platforms can be subdivided into two categories: an open cell electrical biasing platform and a closed electrochemical cell platform. In the open cell configuration, an *in situ* TEM biasing system is used to apply a potential difference between electrodes to induce structural and chemical changes. Specific to Li-ion battery research, structural changes in SnO_2 nanowire electrodes have been studied during Li intercalation in experiments facilitated by the use of TEM vacuum-compatible, ionic liquid-based electrolytes as a medium for Li-ion transport.[49,50] Organic and aqueous based electrolytes have a high vapor pressure and would readily evaporate when placed in the high vacuum environment of the electron microscope; therefore, an alternative method has been developed.

In situ liquid cell microscopy is a rapidly emerging *in situ* S/TEM based characterization technique that allows for the direct imaging and analysis of liquid phase phenomena at high spatial and temporal resolution.[19] This method utilizes microfabricated silicon microchip devices to encapsulate thin layers of liquid electrolyte between electron transparent silicon nitride membranes. The entire assembly is contained within vacuum-tight *in situ* TEM holders. The silicon nitride membranes provide an electron transparent media through which evolving chemical processes within a liquid environment can be directly imaged and analyzed. Modification of the liquid cell microchip platform with microelectrodes has opened a new pathway to investigate electrochemical processes in a technique termed *in situ* electrochemical S/TEM (*In situ* ec-S/TEM). Here the "on-chip" microelectrodes are interfaced with electrical biasing contacts that are embedded within the tip of the vacuum-tight *in situ* TEM holders, which are in turn interfaced with a potentiostat for electroanalytical studies. The electrochemical microchip devices along with the *in situ* TEM holder can be seen in Fig. 4 a-d.

With this system, the reactions kinetics and mechanisms of electrochemical processes have been explored. For example, Unocic *et al*.[51] have applied several electroanalytical techniques (cyclic voltammetry, chronamperomety, and electrochemical impedance spectroscopy to demonstrate how quantitative electrochemical measurements can be performed using these microfluidic electrochemical cells with microfabricated microelectrodes using a ferri-ferrocyanide redox reaction couple. They also showed that the results could be quantitatively analyzed and compared with well-established theories in electrochemistry. Additional electrochemical studies using this approach have elucidated dynamics of metal nanoparticle nucleation and growth under galvanostatic electrodepositon conditions, which were then compared with electrochemical nucleation rate theory.[52,53] Similar studies have been used to investigate the electrodeposition of Ni films from an aqueous $NiCl_2$ electrolyte and Pb dendrites from an aqueous $Pb(NO_3)_2$ electrolyte under constant potential.[54,55] Related to lithium ion battery research, this technique has recently been used to visualize the lithiation and delithiation of silicon nanowires,[56] to track ionic transport in $LiFePO_4$[57] and to investigate the nucleation and growth mechanisms of the solid electrolyte interphase (SEI) layer in lithium ion batteries[46] using organic battery electrolytes as shown in Fig. 4e.

This article summarizes some recent advances in electron microscopy based studies of electrochemical processes in solids and at solid-liquid and solid-gas interfaces. STEM/EELS directly probes a broad range of parameters related to the electrochemical state of the system, including local atomic configurations, bond length and angles,

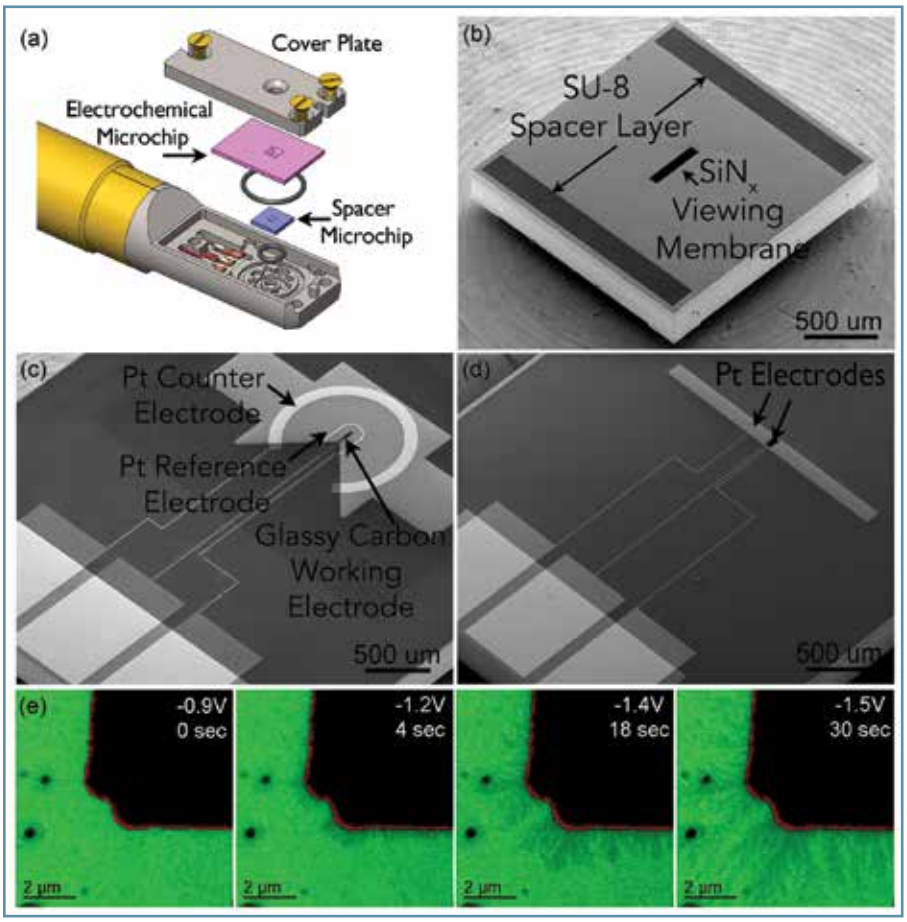

Fig. 4. *(a) Assembly view of in situ electrochemical S/TEM holder which utilizes silicon microchip devices to seal volatile liquid electrolyte between electron transparent SiNx viewing membranes. SEM images of the silicon microchips showing the microfabricated features of the (b) spacer microchip and (c, d) electrochemical microchip.[51] These platforms have been used to study the dynamics of (e) SEI formation on a gold electrode for lithium ion battery studies.[46]*

and valence states and orbital populations of atoms on the individual column level. The challenge in the development of these techniques is now twofold. The first one is common to all S/TEM techniques, which is the continued need for increase in resolution, both spatial (for imaging) and energy (for spectroscopy). With improvements to the current state of the art, electron microscopes will be able to directly probe anisotropic Debye-Waller factors, analyze vibrational modes, and evaluate magnetic states of a single atom. The second challenge is related to electrochemical aspects, and consequently to the necessity to control and probe the local electrochemical potentials and ionic flows in the active region under investigation. This necessitates development of stable electrochemical cells that can support high-resolution studies, while at the same time being able to control global potential and allow local interrogation (*e.g.,* based on SPM) of electrochemical behavior. Some recent results[58-60] suggest that the electron beam can affect the state of materials, offering both an opportunity and a hindrance for probing local electrochemical processes. Finally, of direct interest is the coupling of the local structural and electrochemical behavior into the functionality of a given material under study, and using this information to develop and refine predictive theories. Overall, the combination of STEM/EELS with dynamic electrochemical probing promises to provide an outstanding tool for the exploration of electrochemical systems at hitherto unreachable levels of magnification and resolution.

Acknowledgments

This research was supported in part by the Center for Nanophase Materials Sciences (MC, RRU), which is sponsored at Oak Ridge National Laboratory by the Scientific User Facilities Division, Office of Basic Energy Sciences, U.S. Department of Energy, and also by the Materials Sciences and Engineering Division (AYB), Office of Basic Energy Sciences, U.S. Department of Energy and through user projects supported by Oak Ridge National Laboratory's Center for Nanophase Materials Sciences, which is sponsored at Oak Ridge National Laboratory by the Scientific User Facilities Division, Office of Basic Energy Sciences, U.S. Department of Energy.

About the Authors

Albina Borisevich studied materials science and engineering at the University of Pennsylvania in 1998-2002, focusing in her PhD work on structural studies and solid state chemistry of oxides for microwave applications. She joined the electron microscopy group at Oak Ridge National Laboratory as a postdoctoral fellow in 2002, exploring atomic scale structure of catalysts and new applications of aberration correction such as 3D imaging. Dr. Borisevich became a staff member in 2006 and PI in 2009. Her current research interests encompass atomic-scale mapping of structural distortions in ferroelectric and oxygen conducting oxides, in-situ biasing studies, physics of oxide interfaces, and oxygen vacancy dynamics. She may be reached at albinab@ornl.gov.

Miaofang Chi studied materials science and engineering at the University of California, Davis during 2003-2008. Her PhD research was focused on the investigation of micro-structure-property correlations in complex oxides and the applications of atomic-resolution imaging and spectroscopy to planetary science. She joined the microscopy group at Oak Ridge National Laboratory in 2008 as a research staff member. Her current research is focused on atomic-scale understanding of ionic diffusion behavior at local nanoscale features, such as defects and interfaces, in energy materials. She may be reached at chim@ornl.gov.

Raymond R. Unocic is a R&D Staff Scientist in Oak Ridge National Laboratory's (ORNL's) Center for Nanophase Materials Science Division. Prior to the ORNL appointment, he received his BS in Metallurgical Engineering from the Ohio State University, MS in Materials Science and Engineering from Lehigh University, and PhD in Materials Science and Engineering from the Ohio State University (2008). In 2009 he joined ORNL under the Alvin M. Weinberg Early Career Fellowship then transitioned to Staff Scientist in 2011. His research is focused on the utilization of advanced electron microscopy characterization methods (aberration corrected STEM, HRTEM, EELS, EFTEM, EDS, and *in situ* S/TEM)

(continued on next page)

for materials research. His current research interests are centered on the development and application of novel *in situ* electrochemical S/TEM characterization techniques to probe site-specific electrochemical processes for batteries, fuel cells, and supercapacitors. He may be reached at unocicrr@ornl.gov.

References

1. J. Reed and G. Ceder, *Chemical Reviews,* **104**, 4513 (2004).
2. S. B. Adler, *Chemical Reviews,* **104**, 4791 (2004).
3. A. S. Arico, P. Bruce, B. Scrosati, J.-M. Tarascon, and W. van Schalkwijk, *Nat Mater,* **4**, 366 (2005).
4. R. Erni, M. D. Rossell, C. Kisielowski, and U. Dahmen, *Physical Review Letters,* **102**, 096101 (2009).
5. O. L. Krivanek, *et al., Nature,* **464**, 571 (2010).
6. M. Varela, *et al., Physical Review Letters,* **92**, 095502 (2004).
7. T. C. Lovejoy, *et al., Applied Physics Letters,* **100**, 181602 (2012).
8. M. Bosman, *et al., Physical Review Letters,* **99**, 086102 (2007).
9. Muller, D. A., *et al.* Atomic-Scale Chemical Imaging of Composition and Bonding by Aberration-Corrected Microscopy. *Science* **319**, 1073 (2008).
10. Y. Shao-Horn, L. Croguennec, C. Delmas, E. C. Nelson, and M. A. O'Keefe, *Nat Mater,* **2**, 464 (2003).
11. M. D. Rossell, R. Erni, M. Asta, V. Radmilovic, and U. Dahmen, *Physical Review B,* **80**, 024110 (2009).
12. R. Ishikawa, *et al., Nat Mater,* **10**, 278 (2011).
13. L. H. Wang, Z. Zhang, and X. D. Han, *Npg Asia Materials,* **5**, e40 (2013).
14. H. Nili, K. Kalantar-zadeh, M. Bhaskaran, and S. Sriram, *Progress in Materials Science,* **58**, 1 (2013).
15. A. Gouldstone, *et al., Acta Materialia,* **55**, 4015 (2007).
16. S. R. Zhang, *et al., Accounts of Chemical Research,* **46**, 1731 (2013).
17. J. Y. Liu, *Chemcatchem,* **3**, 934 (2011).
18. P. L. Hansen, S. Helveg, and A. K. Datye, *Advances in Catalysis,* **50**, 77 (2006).
19. N. de Jonge and F. M. Ross, *Nature Nanotechnology,* **6**, 695 (2011).
20. X. L. Tan, H. He, and J. K. Shang, *Journal of Materials Research,* **20**, 1641 (2005).
21. C. T. Nelson, *et al., Science,* **334**, 968 (2011).
22. P. Gao, *et al., Advanced Materials,* **24**, 1106 (2012).
23. P. Gao, *et al., Micron,* **41**, 301 (2010).
24. Y. C. Yang, *et al., Nature Communications,* **3**, 732 (2012).
25. T. Torimoto, T. Tsuda, K. Okazaki, and S. Kuwabata, *Advanced Materials,* **22**, 1196 (2010).
26. C. L. Jia, *et al., Nature Materials,* **7**, 57 (2008).
27. C. L. Jia, *et al., Nature Materials,* **6**, 64 (2007).
28. M. F. Chisholm, W. D. Luo, M. P. Oxley, S. T. Pantelides, and H. N. Lee, *Physical Review Letters,* **105**, 197602 (2010).
29. H. J. Chang, *et al., Advanced Materials,* **23**, 2474 (2011).
30. C. T. Nelson, *et al., Nano Letters,* **11**, 828 (2011).
31. S. B. Adler, *Journal of the American Ceramic Society,* **84**, 2117 (2001).
32. E. V. Tsipis, *et al., Solid State Ionics,* **192**, 42 (2011).
33. Y. M. Kim, *et al., Nat Mater* **11**, 888 (2012).
34. D. N. Leonard, *et al., Advanced Energy Materials,* **3**, 788 (2013).
35. A. Kumar, F. Ciucci, A. N. Morozovska, S. V. Kalinin, and S. Jesse, *Nature Chemistry,* **3**, 707 (2011).
36. Y.-M. Kim, *et al., Nature Materials,* **11**, 888 (2012).
37. K. J. Carroll, *et al., Physical Chemistry Chemical Physics,* **15**, 11128 (2013).
38. C. R. Fell, M. F. Chi, Y. S. Meng, and J. L. Jones, *Solid State Ionics,* **207**, 44 (2012).
39. M. Gu, *et al., Acs Nano,* **7**, 760 (2013).
40. B. Xu, C. R. Fell, M. F. Chi, and Y. S. Meng, *Energy & Environmental Science,* **4**, 2223 (2011).
41. R. Huang, *et al., Applied Physics Letters,* **98**, 051913 (2011).
42. J. W. Lee, W. Zhou, J. C. Idrobo, S. J. Pennycook, and S. T. Pantelides, *Physical Review Letters,* **107**, 085507 (2011).
43. Y. Sun, *et al., Nature Communications,* **4**, 1870 (2013).
44. J. Yao, X. P. Shen, B. Wang, H. K. Liu, and G. X. Wang, *Electrochemistry Communications,* **11**, 1849 (2009).
45. C. Ma, *et al., Energy & Environmental Science,* **7**, 1638 (2014).
46. R. L. Sacci, *et al., Chemical Communications,* **50**, 2104 (2014).
47. P. Abellan, *et al., Nano Letters,* **14**, 1293 (2014).
48. Z. Zeng *et al*., *Nano Letters*, **14** (4), 1745 (2014).
49. J. Y. Huang, *et al., Science,* **330**, 1515 (2010).
50. C.-M. Wang, *et al., Nano Letters,* **11**, 1874 (2011).
51. R. R. Unocic *et al*., *Microscopy & Micro-analysis,* **20**, 442 (2014).
52. M. J. Williamson, R. M. Tromp, P. M. Vereecken, R. Hull, and R. M. Ross, *Nature Materials,* **2**, 532 (2003).
53. A. Radisic, P. M. Vereecken, J. B. Hannon, P. C. Searson, and F. M. Ross, *Nano Letters,* **6**, 238 (2006).
54. X. Chen, K. W. Noh, J. G.Wen, and S. J. Dillon, *Acta Materialia,* **60**, 192 (2012).
55. E. R. White, *et al., Acs Nano,* **6**, 6308 (2012).
56. M. Gu *et al*., *Nano Letters*, **12**, 2318 (2012).
57. M. E. Holtz, *et al*., *Nano Letters* **14**(3), 1453 (2014).
58. P. Y. Huang, *et al., Science,* **342**, 224 (2013).
59. J. Lin, *et al., Nature Nanotechnology,* **in press**, doi:10.1038/nnano.2014.81 (2014).
60. J. H. Jang, *et al.* at http://meetings.aps.org/link/BAPS.2014.MAR.S49.12.